18th IEEE International Conference on Control Applications
Part of 2009 IEEE Multi-conference on Systems and Control
Saint Petersburg, Russia, July 8-10, 2009

A Youla-Kucera approach to Gain-Scheduling with Application to Wind Turbine Control

Michael O.K. Niss, Thomas Esbensen, Christoffer Sloth, Jakob Stoustrup, and Peter F. Odgaard

Abstract— **This paper addresses bumpless transfer between observer-based controllers with integral action in a gain-scheduling architecture with application to wind turbine control. Two methods based on the Youla-Kucera parameterization are applied to achieve bumpless transfer between controllers having equal or different number of control signals and integrators while preserving stability guarantees. Both methods handle reference signals to the controllers.**

The scheduling variable is described by a continuous function, and even in situations where a transfer between two controllers is only initiated but not finalized, stability is sustained and no bumps are introduced in the control signals.

The gain-scheduling approaches are verified by simulation on a non-linear model of a wind turbine.

I. INTRODUCTION

Today, wind energy is the most competitive form of renewable energy. In the past decade the size and capacity of wind turbines have increased dramatically. Meanwhile, the structural components have been made relatively lighter to keep down costs. This has put higher demands on wind turbine control schemes, and implementation of advanced control systems is considered a promising way of decreasing fatigue loads.

In this paper a three-bladed horizontal-axis variable-speed variable-pitch wind turbine is considered, which works from the principle that wind acts on the blades making the rotor shaft rotate. The aerodynamic properties of the wind turbine are affected by the pitch angle of the blades, the speed of the rotor, and the effective wind speed. On this basis, an aerodynamic torque is applied to the rotor and an aerodynamic thrust affects the tower. The aerodynamic torque is transferred to the generator through a drive train in order to upscale the rotational speed of the rotor.

In terms of control, the wind turbine works in two distinct regions. Below a certain wind speed, in the partial load region, the turbine is controlled to generate as much power as possible. This is achieved by adjusting the generator torque to obtain an optimum ratio between the tip speed of the blades and the wind speed. In the full load region the wind turbine is controlled to produce a rated power output, which is obtained by pitching the blades to adjust the efficiency of the rotor.

Various control approaches have been applied in relation to wind turbine control, such as classical control [1], LQ control [2], and robust control [3]. Typically, a control law is calculated based on a linearized plant model at a selected operating point, and is valid only for a narrow range of operation. Gain-scheduling is a natural approach for designing controllers for the entire operating range of the wind turbine, which is based on intersection of several linear controllers designed along a chosen operating trajectory. In [4] and [5] this is done by scheduling parameters according to a scheduling variable, while in [6] and [7] controller switches are performed abruptly.

In this paper two gain-scheduling approaches are presented for performing transitions between controllers of similar or different structures, respectively. The first method is based on [8] while the second method furthermore is inspired by [9]. Both methods provide bumpless transfer between observer-based controllers while maintaining stability guarantees. The approaches are based on the Youla-Kucera parameterization of all stabilizing controllers and were demonstrated on the observer-based robust state-feedback controllers designed for the wind turbine in [10].

This paper is organized as follows. Section II describes the model of the wind turbine. In Section III the considered controllers for the wind turbine are presented for which bumpless transfer is demonstrated. Section IV presents methods for performing bumpless transfer between controllers having identical and different structures. In Section V simulation results are presented, and the paper is finalized by a conclusion in Section VI.

II. WIND TURBINE MODEL

A non-linear model of a wind turbine acts as a simulation model for the proposed control algorithms. The model is based on a static model of the aerodynamics, a two-mass model of the drive train, an electromechanical model of the generator, actuator models, and zero-mean Gaussian distributed measurement noises.

A. Aerodynamic Model

The rotor of the wind turbine converts energy from the wind to the rotor shaft, rotating at the speed $\omega_{\mathrm{r}}(t)$. The power from the wind depends on the wind speed, the air density, ρ, and the swept area, A. From the available power in the swept area, the power on the rotor is given based on the power coefficient, $C_{\mathrm{p}}(\lambda(t), \beta(t))$, which depends on the pitch angle of the blades, $\beta(t)$, and the ratio between the speed of the blade tip and the wind speed, denoted tip-speed ratio, $\lambda(t)$. The aerodynamic torque applied to the rotor by the effective

Michael O.K. Niss, Thomas Esbensen, and Christoffer Sloth are M.Sc. students at Automation and Control, Department of Electronic Systems, Aalborg University, Fredrik Bajers Vej 7C, DK-9220 Aalborg East, Denmark
Jakob Stoustrup is with Automation and Control, Department of Electronic Systems, Aalborg University, DK-9220 Aalborg East, Denmark
Peter F. Odgaard is with kk-electronic a/s, DK-8260 Viby J, Denmark

wind speed passing through the rotor, $v_r(t)$, is given as:

$$T_a(t) = \frac{1}{2\omega_r(t)} \rho A v_r^3(t) C_p(\lambda(t), \beta(t)) \quad [\text{Nm}] \qquad (1)$$

The coefficient C_p describes the aerodynamic efficiency of the rotor by a nonlinear mapping as illustrated in Fig. 1.

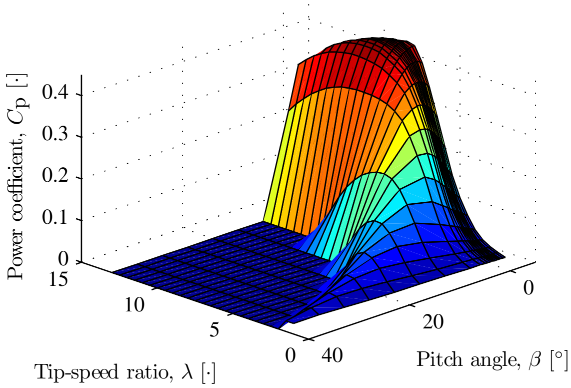

Fig. 1. Illustration of the power coefficient, C_p.

B. Drive Train Model

The drive train model consists of a low-speed shaft and a high-speed shaft having inertias J_r and J_g. The shafts are interconnected by a gear ratio, N_g, combined with torsion stiffness, K_{dt}, and torsion damping, B_{dt}, which result in a torsion angle $\theta_\Delta(t)$. The drive train has efficiency η_{dt} and drives the loading torque from the generator, $T_g(t)$, at a speed $\omega_g(t)$. The linear model is given as:

$$J_r\dot{\omega}_r(t) = T_a(t) - K_{dt}\theta_\Delta(t) - B_{dt}\dot{\theta}_\Delta(t) \quad [\text{Nm}] \qquad (2)$$

$$J_g\dot{\omega}_g(t) = \frac{\eta_{dt}K_{dt}}{N_g}\theta_\Delta(t) + \frac{\eta_{dt}B_{dt}}{N_g}\dot{\theta}_\Delta(t) - T_g(t) \quad [\text{Nm}] \qquad (3)$$

$$\dot{\theta}_\Delta(t) = \omega_r(t) - \frac{1}{N_g}\omega_g(t) \quad [\text{rad/s}] \qquad (4)$$

C. Pitch System Model

The pitch system tracks a reference, $\beta_{ref}(t)$, and is modeled as a first order system. Its time constant is τ, and includes also a communication delay, t_d.

$$\dot{\beta}(t) = -\frac{1}{\tau}\beta(t) + \frac{1}{\tau}\beta_{ref}(t - t_d) \quad [°/\text{s}] \qquad (5)$$

Besides the linear dynamics described by (5), the model also includes constraints on the slew rate and operational range.

D. Generator and Converter Models

Electric power is generated by the generator, while a power converter interfaces the wind turbine generator output with the utility grid and controls the currents in the generator. The generator torque in (6) is adjusted by the reference $T_{g,ref}(t)$. The dynamics of the converter is approximated by a first order system with time constant τ_g and communication delay $t_{g,d}$. Just as for the model of the pitch system, the slew rate and operational range of the converter are limited.

$$\dot{T}_g(t) = -\frac{1}{\tau_g}T_g(t) + \frac{1}{\tau_g}T_{g,ref}(t - t_{g,d}) \quad [\text{Nm/s}] \qquad (6)$$

The power produced by the generator can be approximated from the mechanical power calculated below, where η_g denotes the efficiency of the generator, which is assumed constant.

$$P_g(t) = \eta_g\omega_g(t)T_g(t) \quad [\text{W}] \qquad (7)$$

E. Assembled Model

The interconnection of the wind turbine sub-models is illustrated in Fig. 2. The input to the model is provided by a modified version of the wind model SB-2 in [11], to which the swaying of the tower is added.

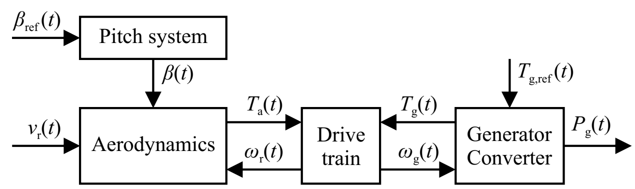

Fig. 2. Block diagram of the wind turbine model.

Available measurements are: generator torque, pitch angle, generator speed, and rotor speed; all sampled at a rate of 100 Hz. The output power is not available as an actual measurement, but is evaluated as the product of the measurements of the generator speed and generator torque. To present the quality of the measurements, these are emulated as deterministic values with addition of zero-mean Gaussian noises with the following standard deviations: $\sigma_{Tg} = 90$ Nm, $\sigma_\beta = 0.2°$, $\sigma_{\omega g} = 0.05$ rad/s, and $\sigma_{\omega r} = 0.025$ rad/s.

F. Model Parameters

The following parameters are chosen such that they represent a realistic but fictitious turbine: $A = 10{,}387$ m^2, $\rho = 1.225$ kg/m^3, $B_{dt} = 9.45$ MNm/(rad/s), $J_r = 55 \cdot 10^6$ kgm^2, $J_g = 390$ kgm^2, $K_{dt} = 2.7$ GNm/rad, $N_g = 95$, $\eta_{dt} = 0.97$, $t_d = 10$ ms, $\tau = 50$ ms, $t_{g,d} = 20$ ms, $\tau_g = 10$ ms, $\eta_g = 0.92$.

III. MIXED SENSITIVITY CONTROLLERS WITH INTEGRAL ACTION

To control the wind turbine a set of four different robust controllers were designed, operating in different regions of the operational area. The designed controllers are described in [10] and are based on robust state feedback controllers combined with optimal observers to provide full state information. The control law of each controller is given as $\boldsymbol{u}(t) = \boldsymbol{F}_c\boldsymbol{x}(t)$.

Two different controller structures exist in order to adjust the controllers to the different objectives in the partial and full-load regions of the wind turbine. These regions are further divided into two, to narrow the parameter uncertainties of a region resulting from the non-linear nature of the aerodynamics.

Each of the controllers has integral states, one for each of the references that need to be followed. For the controllers utilized in partial load operation, i.e. in Region 1 and 2, there exists only a reference to the generator speed, $\omega_g(t)$. For the controllers in full load operation, i.e. in Region 3 and 4, an additional reference exist to the output power, $P_g(t)$.

In the design of the controllers a mixed sensitivity description was utilized in order to specify performance requirements. This resulted in additional states in the control formulation originating from the introduced weight filters; these are denoted W. Note that $\tau(t)$ represents the state of a first order Padé approximation and an 'e' in the index denotes the innovation of the given variable.

The states utilized in the controllers in Region 1 and 2 are: $T_g(t)$, $\theta_\Delta(t)$, $\omega_g(t)$, $\omega_r(t)$, $\int \omega_{g,e}(t)dt$, $v_r(t)$, $\omega_{g,ref}(t)$, $\tau_{Tg}(t)$, $W_{\omega g}(t)$, $W_{\int \omega g,e}(t)$, and $W_{Tg,ref}(t)$.
For the controllers in Region 3 and 4 the following additional states are included: $\beta(t)$, $\int P_{g,e}(t)dt$, $P_{g,ref}(t)$, $\tau_\beta(t)$, $W_{Pg}(t)$, $W_{\int Pg,e}(t)$, $W_{\beta ref}(t)$, and $W_{\dot{\beta} ref}(t)$.

IV. BUMPLESS TRANSFER METHODS

In a transition between different controllers it is desirable to ensure a bumpless transfer while maintaining stability guarantees. This paper presents two methods which fulfill this requirement; one method that enables transitions between controllers having identical structures, and another method for making transitions between controllers having structural differences. Note that both methods assume sufficiently slow transitions.

Both of the presented gain-scheduling methods are based on the Youla-Kucera parameterization, but are applicable in different situations. The first method was used for scheduling between controllers with similar structures and is an extension of the method presented in [8], [12], and [13]. The extension was made in order to include references and disturbances in the wind turbine controller and to enable filtering of the integral states. The second method addresses the transitions between different controller structures. It utilizes some principals from the first method and is also inspired by [9] to utilize Youla-Kucera parameterization in another way.

The methods based on the Youla-Kucera parameterization were chosen as they, in contrast to a simple weighting of the control signals from two or more controllers, guarantees stability for all values of the scheduling variable $\alpha \in [0; 1]$, as discussed in [13].

Scheduling Between Controllers with Similar Structures

The method established in [8], [12], and [13] assumes that two different linearizations of a system is available, each valid in different, but overlapping, operating ranges:

$$\left[\begin{array}{c|c} \boldsymbol{A}_1 & \boldsymbol{B}_1 \\ \hline \boldsymbol{C}_1 & \boldsymbol{0} \end{array}\right] \text{ and } \left[\begin{array}{c|c} \boldsymbol{A}_2 & \boldsymbol{B}_2 \\ \hline \boldsymbol{C}_2 & \boldsymbol{0} \end{array}\right]$$

If the system is detectable and stabilizable, which holds for the wind turbine model considered in this paper, an observer-based controller can be designed. No matter which design approach that has been used, a resulting controller can always be put on a form where $\boldsymbol{F}_1$ and $\boldsymbol{F}_{I1}$ describe the state and integral state feedback matrices. Additionally, $\boldsymbol{S}_1$ is a matrix that picks out the signals to be integrated and $\boldsymbol{L}_1$ is the observer gain matrix. The resulting controller can be described as:

$$\boldsymbol{K}_1(s) = \left[\begin{array}{cc|c} \boldsymbol{A}_1 + \boldsymbol{B}_1\boldsymbol{F}_1 + \boldsymbol{L}_1\boldsymbol{C}_1 & \boldsymbol{B}_1\boldsymbol{F}_{I1} & \text{-}\boldsymbol{L}_1 \\ \boldsymbol{0} & \boldsymbol{0} & \boldsymbol{S}_1 \\ \hline \boldsymbol{F}_1 & \boldsymbol{F}_{I1} & \boldsymbol{0} \end{array}\right] \tag{8}$$

A system set up in the block form written above corresponds to the observer-based controller described by the following equations, where $\boldsymbol{x}_1(t)$ and $\boldsymbol{x}_{I1}(t)$ are the observer and integral states, whereas $\boldsymbol{u}(t)$ and $\boldsymbol{y}(t)$ are the control signal and measured output:

$$\begin{aligned} \dot{\boldsymbol{x}}_1(t) &= \boldsymbol{A}_1\boldsymbol{x}_1(t) + \boldsymbol{B}_1\left(\boldsymbol{F}_1\boldsymbol{x}_1(t) + \boldsymbol{F}_{I1}\boldsymbol{x}_{I1}(t)\right) \\ &\quad + \boldsymbol{L}_1\left(\boldsymbol{C}_1\boldsymbol{x}_1(t) - \boldsymbol{y}(t)\right) && \text{(9a)} \\ \dot{\boldsymbol{x}}_{I1}(t) &= \boldsymbol{S}_1\boldsymbol{y}(t) && \text{(9b)} \\ \boldsymbol{u}(t) &= \boldsymbol{F}_1\boldsymbol{x}_1(t) + \boldsymbol{F}_{I1}\boldsymbol{x}_{I1}(t) && \text{(9c)} \end{aligned}$$

Since an integral state results in a pole in zero for the open-loop system, it has to be treated with special care in the considered gain-scheduling method. This is why $\boldsymbol{F}_{I1}$ is separated from the rest of the feedback gains contained in $\boldsymbol{F}_1$.

To be able to use the gain-scheduling method presented here, the controller must be able to stabilize the system. This is fulfilled if and only if the following matrices are Hurwitz:

$$[\boldsymbol{A}_1 + \boldsymbol{L}_1\boldsymbol{C}_1] \text{ and } \left[\begin{array}{cc} \boldsymbol{A}_1 + \boldsymbol{B}_1\boldsymbol{F}_1 & \boldsymbol{B}_1\boldsymbol{F}_{I1} \\ \boldsymbol{S}_1\boldsymbol{C}_1 & \boldsymbol{0} \end{array}\right]$$

The Youla-Kucera parameterization lets a controller be implemented as a function of a stable system, $\boldsymbol{Q}(s)$, based on another stabilizing controller, $\boldsymbol{\mathcal{K}}_1(s)$. The interconnection of the systems is shown in Fig. 3. As stated in [14] this implies that it is possible to transfer between two controllers online in a bumpless manner, without compromising stability, by scaling the $\boldsymbol{Q}(s)$ system by a factor $\alpha \in [0; 1]$, e.g. from the controller $\boldsymbol{K}_1(s)$ to the next controller $\boldsymbol{K}_2(s)$.

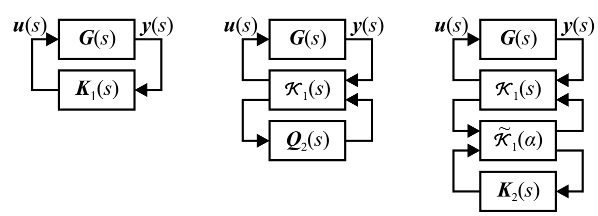

Fig. 3. Left: Interconnection between the system $\boldsymbol{G}(s)$ and the controller $\boldsymbol{K}_1(s)$. Middle: Controller implemented as $\boldsymbol{K}_1(\boldsymbol{Q}_2(s)) = \boldsymbol{\mathcal{K}}_1(s) \star \boldsymbol{Q}_2(s)$. Right: $\boldsymbol{Q}_2(s)$ is given as $\tilde{\boldsymbol{\mathcal{K}}}_1(\alpha) \star \boldsymbol{K}_2(s)$.

To form the system necessary to perform the scheduling, the control system matrix in (8) is extended into (11) and (12). The system in (11) is the original stabilizing controller, $\boldsymbol{K}_1(s)$, extended with interconnections for a Youla-Kucera parameterization, $\boldsymbol{Q}(s)$, while the system in (12) is designed to fulfill the following equation:

$$\boldsymbol{\mathcal{K}}_1(s) \star \tilde{\boldsymbol{\mathcal{K}}}_1(\alpha) \star \boldsymbol{K}_2(s) \triangleq \boldsymbol{K}_2(s) \quad \text{for } \alpha = 1 \tag{10}$$

A multi-port system on block form should be interpreted such that if Fig. 3 is related to (11), the first input column in the block system corresponds to the uppermost input in the figure, the second column to the next input in line, etc. Exactly the same applies to the outputs.

In the following equations the tuning parameter r determines how far into the left half plane the poles of the integrators of $\tilde{\mathcal{K}}_1(\alpha)$ should be moved. The constraints $r > 0$ and $\boldsymbol{W}_1\boldsymbol{F}_{\mathrm{I1}} = r\boldsymbol{I}$ should be satisfied.

$$\mathcal{K}_1(s) = \left[\begin{array}{cc|cc} \boldsymbol{A}_1+\boldsymbol{B}_1\boldsymbol{F}_1+\boldsymbol{L}_1\boldsymbol{C}_1 & \boldsymbol{B}_1\boldsymbol{F}_{\mathrm{I1}} & -\boldsymbol{L}_1 & \boldsymbol{B}_1 \\ \boldsymbol{0} & \boldsymbol{0} & \boldsymbol{S}_1 & \boldsymbol{W}_1 \\ \hline \boldsymbol{F}_1 & \boldsymbol{F}_{\mathrm{I1}} & \boldsymbol{0} & \boldsymbol{I} \\ \boldsymbol{C}_1 & \boldsymbol{0} & -\boldsymbol{I} & \boldsymbol{0} \end{array}\right] \tag{11}$$

$$\tilde{\mathcal{K}}_1(\alpha) = \left[\begin{array}{cc|cc} \boldsymbol{A}_1 & \boldsymbol{0} & \boldsymbol{L}_1 & \boldsymbol{B}_1 \\ \boldsymbol{S}_1\boldsymbol{C}_1-\boldsymbol{W}_1\boldsymbol{F}_1 & -r\boldsymbol{I} & -\boldsymbol{S}_1 & \boldsymbol{W}_1 \\ \hline -\alpha\boldsymbol{F}_1 & -\alpha\boldsymbol{F}_{\mathrm{I1}} & \boldsymbol{0} & \alpha\boldsymbol{I} \\ \boldsymbol{C}_1 & \boldsymbol{0} & -\boldsymbol{I} & \boldsymbol{0} \end{array}\right] \tag{12}$$

The matrices specified in (11), (12), and (8) have the following properties, which enable bumpless transfer between the controllers $\boldsymbol{K}_1(s)$ and $\boldsymbol{K}_2(s)$:

- For $\alpha = 0$ the following holds: $\mathcal{K}_1(s) \star \tilde{\mathcal{K}}_1(\alpha) \star \boldsymbol{K}_2(s) \stackrel{\Delta}{=} \boldsymbol{K}_1(s)$, i.e. the resulting controller is $\boldsymbol{K}_1(s)$.
- For $\alpha = 1$ the following holds: $\mathcal{K}_1(s) \star \tilde{\mathcal{K}}_1(\alpha) \star \boldsymbol{K}_2(s) \stackrel{\Delta}{=} \boldsymbol{K}_2(s)$, i.e. the resulting controller is $\boldsymbol{K}_2(s)$.
- The poles of the closed loop system are, for all α, identical to the eigenvalues of the matrices listed below.

$$\left[\begin{array}{cc} \boldsymbol{A}_1+\boldsymbol{B}_1\boldsymbol{F}_1 & \boldsymbol{B}_1\boldsymbol{F}_{\mathrm{I1}} \\ \boldsymbol{S}_1\boldsymbol{C}_1 & \boldsymbol{0} \end{array}\right]$$
$$\left[\begin{array}{cc} \boldsymbol{A}_2+\boldsymbol{B}_2\boldsymbol{F}_2 & \boldsymbol{B}_2\boldsymbol{F}_{\mathrm{I2}} \\ \boldsymbol{S}_2\boldsymbol{C}_2 & \boldsymbol{0} \end{array}\right]$$
$$[\boldsymbol{A}_1+\boldsymbol{L}_1\boldsymbol{C}_1], \quad [\boldsymbol{A}_2+\boldsymbol{L}_2\boldsymbol{C}_2], \quad -r\boldsymbol{I}$$

Let x_1 and $\tilde{x}_1$ denote the states in $\mathcal{K}_1(s)$ and $\tilde{\mathcal{K}}_1(\alpha)$ respectively, then if α has been 1 for some time the states $\tilde{x}_1$ will converge to x_1, at a rate given by the eigenvalues of the following matrix. This is explained in [13] and is independent of the input signal.

$$\left[\begin{array}{cc} \boldsymbol{A}_1+\boldsymbol{B}_1\boldsymbol{F}_1 & \boldsymbol{B}_1\boldsymbol{F}_{\mathrm{I1}} \\ \boldsymbol{S}_1\boldsymbol{C}_1 & \boldsymbol{0} \end{array}\right]$$

To adapt the gain-scheduling method to the considered wind turbine model, it was necessary to adjust the matrices presented so far. The reason is that references and disturbances had to be added to the general model. Also, some changes had to be made since it must be ensured that the integral states of the controller can be filtered, as required by the mixed sensitivity design method.

The state feedback matrix, $\boldsymbol{F}_{\mathrm{c}}$, for each of the controllers, is divided into three matrices. When written for Controller 1 this means that $\boldsymbol{F}_{\mathrm{I1}}$ holds the gains concerning the integral states, $\boldsymbol{F}_{\mathrm{d1}}$ holds the gains concerning the references and disturbances, i.e. $\omega_{\mathrm{g,ref}}(t)$, $P_{\mathrm{g,ref}}(t)$, and $v_{\mathrm{r}}(t)$, while $\boldsymbol{F}_1$ consists of the remaining gains.

For including the disturbances into the systems an extra input column was added to the system descriptions, $\mathcal{K}_1(s)$, $\tilde{\mathcal{K}}_1(\alpha)$, and $\boldsymbol{K}_2(s)$, and an extra row was added to the systems for them to pass on the disturbances to the interconnected systems. Additionally, to reduce influence from measurement noise on the control output, the system descriptions were modified so that the estimated states are integrated instead of the measurements.

The controller presented in (8) is rewritten into (15), presented as $\boldsymbol{K}_2(s)$ instead. In a similar manner $\mathcal{K}_1(s)$ and $\tilde{\mathcal{K}}_1(\alpha)$ are modified to include the additions. They are presented in (13) and (14). The systems in (13), (14), and (15) enable transitions between controllers having identical structures, including references and disturbances.

$$\mathcal{K}_1(s) = \left[\begin{array}{cc|ccc} \boldsymbol{A}_1+\boldsymbol{B}_1\boldsymbol{F}_1+\boldsymbol{L}_1\boldsymbol{C}_1 & \boldsymbol{B}_1\boldsymbol{F}_{\mathrm{I1}}+\boldsymbol{B}_{\mathrm{I1}} & -\boldsymbol{L}_1 & \boldsymbol{B}_{\mathrm{d1}}+\boldsymbol{B}_1\boldsymbol{F}_{\mathrm{d1}} & \boldsymbol{B}_1 \\ \boldsymbol{S}_1\boldsymbol{C}_1 & \boldsymbol{0} & \boldsymbol{0} & -\boldsymbol{N}_{\mathrm{d1}} & \boldsymbol{W}_1 \\ \hline \boldsymbol{F}_1 & \boldsymbol{F}_{\mathrm{I1}} & \boldsymbol{0} & \boldsymbol{F}_{\mathrm{d1}} & \boldsymbol{I} \\ \boldsymbol{C}_1 & \boldsymbol{0} & -\boldsymbol{I} & \boldsymbol{0} & \boldsymbol{0} \\ \boldsymbol{0} & \boldsymbol{0} & \boldsymbol{0} & \boldsymbol{I} & \boldsymbol{0} \end{array}\right] \tag{13}$$

$$\tilde{\mathcal{K}}_1(\alpha) = \left[\begin{array}{cc|ccc} \boldsymbol{A}_1 & \boldsymbol{B}_{\mathrm{I1}} & \boldsymbol{L}_1 & \boldsymbol{B}_{\mathrm{d1}} & \boldsymbol{B}_1 \\ \boldsymbol{S}_1\boldsymbol{C}_1-\boldsymbol{W}_1\boldsymbol{F}_1 & -r_1\boldsymbol{I} & \boldsymbol{0} & -\boldsymbol{N}_{\mathrm{d1}}-\boldsymbol{W}_1\boldsymbol{F}_{\mathrm{d1}} & \boldsymbol{W}_1 \\ \hline -\alpha\boldsymbol{F}_1 & -\alpha\boldsymbol{F}_{\mathrm{I1}} & \boldsymbol{0} & -\alpha\boldsymbol{F}_{\mathrm{d1}} & \alpha\boldsymbol{I} \\ \boldsymbol{C}_1 & \boldsymbol{0} & -\boldsymbol{I} & \boldsymbol{0} & \boldsymbol{0} \\ \boldsymbol{0} & \boldsymbol{0} & \boldsymbol{0} & \boldsymbol{I} & \boldsymbol{0} \end{array}\right] \tag{14}$$

$$\boldsymbol{K}_2(s) = \left[\begin{array}{cc|cc} \boldsymbol{A}_2+\boldsymbol{B}_2\boldsymbol{F}_2+\boldsymbol{L}_2\boldsymbol{C}_2 & \boldsymbol{B}_2\boldsymbol{F}_{\mathrm{I2}}+\boldsymbol{B}_{\mathrm{I2}} & -\boldsymbol{L}_2 & \boldsymbol{B}_{\mathrm{d2}}+\boldsymbol{B}_2\boldsymbol{F}_{\mathrm{d2}} \\ \boldsymbol{S}_2\boldsymbol{C}_2 & \boldsymbol{0} & \boldsymbol{0} & -\boldsymbol{N}_{\mathrm{d2}} \\ \hline \boldsymbol{F}_2 & \boldsymbol{F}_{\mathrm{I2}} & \boldsymbol{0} & \boldsymbol{F}_{\mathrm{d2}} \end{array}\right] \tag{15}$$

where:

$\boldsymbol{B}_{\mathrm{d1}}$ and $\boldsymbol{B}_{\mathrm{d2}}$	are matrices which feed the disturbances into the system states
$\boldsymbol{B}_{\mathrm{I1}}$ and $\boldsymbol{B}_{\mathrm{I2}}$	are matrices that feed the state values of the integrators into the output filter states
$\boldsymbol{F}_{\mathrm{d1}}$ and $\boldsymbol{F}_{\mathrm{d2}}$	are matrices which are parts of the state feedback matrices, $\boldsymbol{F}_{\mathrm{c1}}$ and $\boldsymbol{F}_{\mathrm{c2}}$
$\boldsymbol{N}_{\mathrm{d1}}$ and $\boldsymbol{N}_{\mathrm{d2}}$	are matrices that, together with $\boldsymbol{S}_1$ and $\boldsymbol{S}_2$, ensure that the errors according to the references are integrated

Scheduling Between Controllers with Different Structures

The following method allows for scheduling between controllers with different structures. For the considered wind turbine system the controllers in partial load operation only have a reference to the generator speed, while the controllers in full load operation have references to both the generator speed and the output power, which results in a different structure of the controllers. Fig. 4 illustrates the controller structure for this proposed gain-scheduling method.

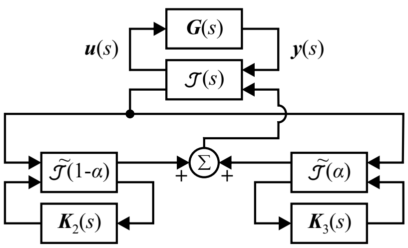

Fig. 4. The structure of the controller used in the scheduling between partial load operation and full load operation, i.e. between Region 2 and 3.

The main difference between the proposed method and the one presented in the last subsection is that scheduling will happen between two different Youla-Kucera parameterizations, $\boldsymbol{Q}_1(s)$ and $\boldsymbol{Q}_2(s)$, instead of scheduling between a stable $\boldsymbol{Q}(s)$ as extension to the active controller and the active controller itself.

When operating the robust controller in the region prior to a transition, i.e. at $\alpha = 0$, the controller will be given as shown below, where $\boldsymbol{\mathcal{J}}(s)$ and $\tilde{\boldsymbol{\mathcal{J}}}(\alpha)$ are systems set up in the same manner as in (11) and (12) respectively.

$$\boldsymbol{K}_2(s) = \boldsymbol{\mathcal{J}}(s) \star \left(\tilde{\boldsymbol{\mathcal{J}}}(1-\alpha) \star \boldsymbol{K}_2(s) + \tilde{\boldsymbol{\mathcal{J}}}(\alpha) \star \boldsymbol{K}_3(s)\right) \tag{16}$$

The idea of the proposed method is that since $\boldsymbol{\mathcal{J}}(s)$ never becomes the active controller it can be designed freely, as long as it is capable of stabilizing the system. The controller $\boldsymbol{\mathcal{J}}(s)$ is merely an intermediate segment between the system and either the controller $\boldsymbol{K}_2(s)$ for $\alpha = 0$, the controller $\boldsymbol{K}_3(s)$ for $\alpha = 1$, or a combination of both controllers.

The advantage of this method is that, although the controllers have different structures, almost the same approach can be utilized as for the first presented method. The constraint is though that $\tilde{\boldsymbol{\mathcal{J}}}(1-\alpha) \star \boldsymbol{K}_2(s)$ and $\tilde{\boldsymbol{\mathcal{J}}}(\alpha) \star \boldsymbol{K}_3(s)$ need to be stable systems, which is easily obtained by the method described in the previous subsection, when $\boldsymbol{\mathcal{J}}(s)$ is designed to be a stabilizing controller.

Handling Operating Points

As the controllers were designed for different linearizations of the system they rely on different operating points. Hence, it was necessary to compensate for these differences when scheduling between the different controllers.

[13] proposes that a simple weighting of the steady-state contribution of each active controller is added to the small signal output of the controllers. This method was however shown to be ineffective for the considered system, as it requires a long scheduling time for the integrators to attain the correct compensation for the changed steady-state values. Instead, another approach was utilized where each signal was changed into an associated large signal value at the output, but was again adjusted into a small signal value fitting the next system that it enters. As illustrated in Fig. 5 compensation is needed in four places, but entails no problem since it is only a matter of adding values to some signals.

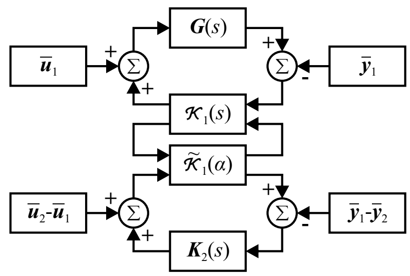

Fig. 5. The structure used for handling operating points.

V. SIMULATION RESULTS

Simulations were performed in MATLAB Simulink to verify the performance of the designed gain-scheduling methods. In the implementation of the gain-scheduling methods, the scheduling variable was implemented as an arcus tangent function around the intended transition point, which appears from the subplots showing the scheduling variable. In partial load operation the scheduling variable depends on the generator speed, in full load operation it depends on the pitch angle, and in the transitions between the partial and full load regions it is a combination of both.

Scheduling Between Controllers with Similar Structures

Fig. 6 shows that a transition from Controller 2 to Controller 1, i.e. between controllers of similar structures, imposed no noticeable disturbance on the control signal; hence, neither on the output. Several transitions were studied in the evaluation of the method, and even in situations where a transfer between two controllers was only initiated but not finalized, the method behaved properly, as dictated by the design. This is apparent in the figure around $t = 110$ s. Notice that the zoom in the figure is adjusted to capture the two different types of transitions.

Scheduling Between Controllers with Different Structures

Fig. 7 shows a transition from Controller 2 to Controller 3, i.e. between controllers of different structures, in the sense of the number of control signals and integrators. When a transition was performed into the full load region, caused by an increasing wind speed, the controller started pitching the blades out of the wind and kept the generator torque around a constant value, as expected. This change in control strategy is apparent from the figure.

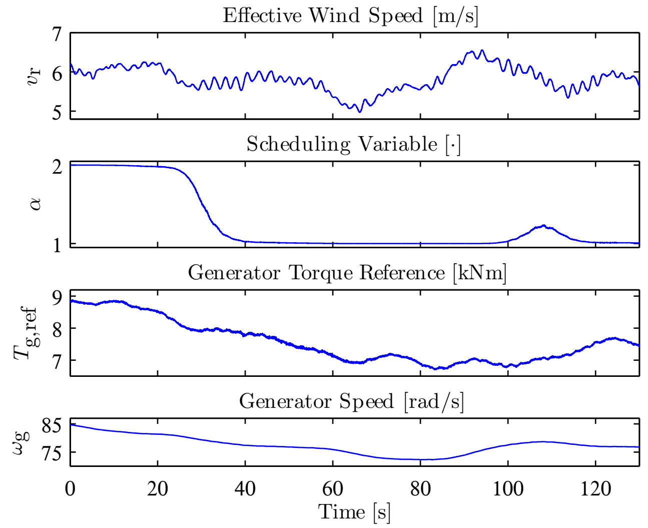

Fig. 6. Evaluation of the gain-scheduling method between controllers having identical structures. When the scheduling variable is equal to 1 the wind turbine is operated by the controller for Region 1, when it is equal to 2 the active controller is the one for Region 2, and for all values in between it is a combination of both.

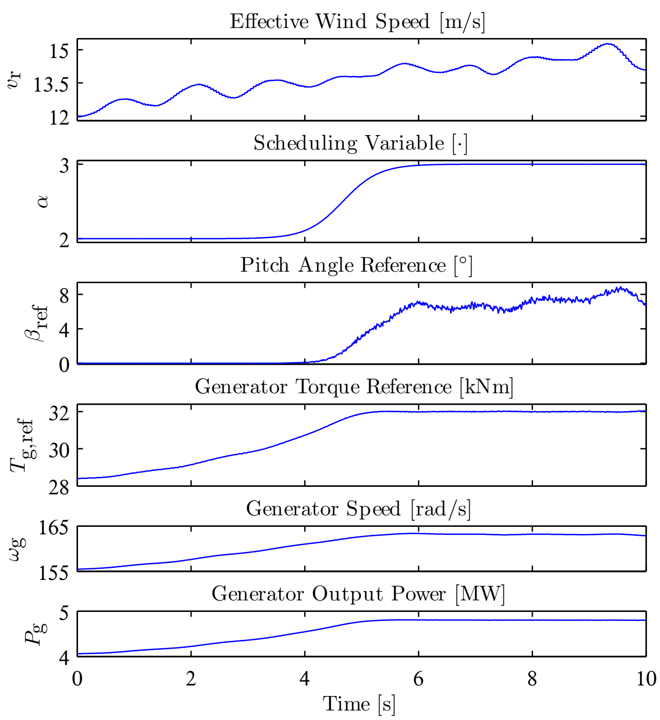

Fig. 7. Evaluation of the gain-scheduling method between controllers having different structures.

VI. CONCLUSION

This paper presents a successful extension to the gain-scheduling method presented in [8], which is applied to a variable-speed variable-pitch wind turbine in the transitions between controllers having identical structures. The method is extended to include references and disturbances to the system and to allow filtering of the integral states.

A gain-scheduling method to be applied for scheduling between controllers having different structures is also proposed. In relation to wind turbine control this is applicable in the transition between the controllers in the partial and full load regions, as these have different numbers of control signals and integrators. The method is developed upon the first method presented and is inspired by [9].

The two methods are verified to allow bumpless transfers between the controllers in the wind turbine system.

REFERENCES

[1] M. Rasila, ”Torque- and Speed Control of a Pitch Regulated Wind Turbine”, *Master’s Thesis*, Department of Electric Power Engineering, Chalmers University of Technology, 2003.

[2] N.K. Poulsen, T.J. Larsen, and M.H. Hansen, ”Comparison between a PI and LQ-regulation for a 2 MW wind turbine”, *Tech. Rep.*, Risø National Laboratory, 2005.

[3] N.A. Cutululis, E. Ceanga, A.D. Hansen, and P. Sørensen, ”Robust multi-model control of an autonomous wind power system”, *Wind Energy*, vol. 9, issue 5, MAR 2006, pp. 399-419.

[4] K. Hammerum, ”A fatigue approach to wind turbine control”, *Master’s Thesis*, Technical University of Denmark, 2006.

[5] P. Sørensen, A.D. Hansen, F. Iov, F. Blaabjerg, and M.H. Donovan, ”Wind farm models and control strategies”, *Tech. Rep.*, Risø National Laboratory, AUG 2005.

[6] I. Kraan and P.M.M. Bongers, ”Control of a wind turbine using several linear robust controllers”, In *Proceedings of the 32th IEEE Conference on Decision and Control*, San Antonio, USA, DEC 1993, pp. 1928-1929.

[7] D.J. Leith and W.E Leithead, ”Performance enhancement of wind turbine power regulation by switched linear control”, *International Journal of Control*, vol. 65, issue 4, NOV 1996, pp. 555-572.

[8] K. Trangbaek, J. Stoustrup, and J.D. Bendtsen, ”Gain Scheduling of Observer-Based Controllers with Integral Action”, In *Proceedings of the 45th IEEE Conference on Decision and Control*, San Diego, USA, DEC 2006, pp. 1393-1398.

[9] D. Alazard and P. Apkarian, ”Exact Observer-based Structures for Arbitrary Compensators”, *International Journal of Robust and Nonlinear Control*, vol. 9, no. 2, 1999, pp. 101-118.

[10] C. Sloth, T. Esbensen, M.O.K. Niss, J. Stoustrup, and P.F. Odgaard, ”Robust LMI-Based Control of Wind Turbines with Parametric Uncertainties”, In *Proceedings of the 3rd IEEE Multi-conference on Systems and Control*, Saint Petersburg, Russia, JUL 2009.

[11] Aalborg University and Risø National Laboratory, Wind Turbine Blockset, 2005, http://www.iet.aau.dk/Research/research_prog/wind_turbine/Projects/SimPlatformPrj/.

[12] J.D. Bendtsen, J. Stoustrup, and K. Trangbaek, ”Bumpless Transfer Between Advanced Controllers with Applications to Power Plant Control”, In *Proceedings of the 42nd IEEE Conference on Decision and Control*, Maui, Hawaii USA, DEC 2003, pp. 2059-2064.

[13] J.D. Bendtsen, J. Stoustrup, and K. Trangbaek, ”Bumpless Transfer Between Observer-Based Gain Scheduled Controllers”, *International Journal of Control*, vol. 78, no. 7, 2005, pp. 491-504.

[14] H. Niemann, and J. Stoustrup, ”An Architecture for Implementation of Multivariable Controllers”, In *Proceedings of the American Control Conference*, San Diego, California, vol. 6, 1999, pp. 4029-4033.